

Thermal noise induced probability switching in magnetic tunnel junction based on spin-circuit simulation

Shaojie Hu(胡少杰), Fupeng Gao(高福朋), Tengwei Huang(黄腾伟), Zhizhong Wang(王志忠), Hui Li(李惠), Dawei Wang(王大威)

Citation: Chin. Phys. B. 35, 098504 (2026). DOI: 10.1088/1674-1056/ae2ebe |
CSTR: 32038.14.CPB.ae2ebe
http://cpb.iphy.ac.cn; http://iopscience.iop.org/cpb

What follows is a list of articles you may be interested in

Improvement of energy resolution of x-ray transition-edge sensor using K-means algorithm and Wiener filter

Qingxiao Ma(马卿效), Wen Zhang(张文), Peizhan Li(李佩展), Zheng Wang(王争), Zhifa Feng(冯志发), Xinkai Yang(杨心开), Jiaqiang Zhong(钟家强), Wei Miao(缪巍), Yuan Ren(任远), Jing Li(李婧), Shengcai Shi(史生才)
Chin. Phys. B. 32, 108501 (2023). DOI: 10.1088/1674-1056/acd7d4

Dark count in single-photon avalanche diodes: A novel statistical behavioral model

Wen-Juan Yu(喻文娟), Yu Zhang(张钰), Ming-Zhu Xu(许明珠), Xin-Miao Lu(逯鑫淼)
Chin. Phys. B. 29, 048503 (2020). DOI: 10.1088/1674-1056/ab7808

Responsivity and noise characteristics of AlGaN/GaN-HEMT terahertz detectors at elevated temperatures

Zhi-Feng Tian(田志锋), Peng Xu(徐鹏), Yao Yu(余耀), Jian-Dong Sun(孙建东), Wei Feng(冯伟), Qing-Feng Ding(丁青峰), Zhan-Wei Meng(孟占伟), Xiang Li(李想), Jin-Hua Cai(蔡金华), Zhong-Xin Zheng(郑中信), Xin-Xing Li(李欣幸), Lin Jin(靳琳), Hua Qin(秦华), Yun-Fei Sun(孙云飞)
Chin. Phys. B. 28, 058501 (2019). DOI: 10.1088/1674-1056/28/5/058501

Development of long-wavelength infrared detector and its space-based application requirements

Junku Liu(刘军库), Lin Xiao(肖林), Yang Liu(刘阳), Longfei Cao(曹龙飞), Zhengkun Shen(申正坤)
Chin. Phys. B. 28, 028504 (2019). DOI: 10.1088/1674-1056/28/2/028504

Damage effect and mechanism of the GaAs high electron mobility transistor induced by high power microwave

Yang Liu(刘阳), Chang-Chun Chai(柴常春), Yin-Tang Yang(杨银堂), Jing Sun(孙静), Zhi-Peng Li(李志鹏)
Chin. Phys. B. 25, 048504 (2016). DOI: 10.1088/1674-1056/25/4/048504

Thermal noise induced probability switching in magnetic tunnel junction based on spin-circuit simulation

Shaojie Hu(胡少杰)[1,†], Fupeng Gao(高福朋)[2], Tengwei Huang(黄腾伟)[1], Zhizhong Wang(王志忠)[1], Hui Li(李惠)[1], and Dawei Wang(王大威)[2]

[1] *Engineering Research Center of Guangdong for Compound Semiconductor Devices and Chips, College of Integrated Circuits and Optoelectronic Chips, Shenzhen Technology University, Shenzhen* 518118, *China*

[2] *School of Microelectronics & State Key Laboratory for Mechanical Behavior of Materials, Xi'an Jiaotong University, Xi'an* 710049, *China*

(Received 10 September 2025; revised manuscript received 17 December 2025; accepted manuscript online 18 December 2025)

The probability switching characteristics in spin transfer torque magnetic tunnel junctions (STT-MTJs) are simulated by considering thermal noise using a spin-circuit module. Thermal noise significantly affects the probability switching for pulse durations exceeding 10 ns, while no probability switching properties are observed for pulses shorter than 1 ns due to precessional switching. For pulse durations between 1 ns and 10 ns, the occurrence of mixed probability and abrupt switching suggests that thermal noise partially influences the switching properties. These results demonstrate the effectiveness of our simulation model in capturing the MTJ properties under the influence of thermal noise. The spin-circuit module used in this study lays the groundwork for future circuit system designs utilizing MTJ devices, such as true random number generators and neural network computing.

Keywords: thermal noise, probability switching, magnetic tunnel junction (MTJ), spin-circuit

PACS: 85.75.Dd

DOI: 10.1088/1674-1056/ae2ebe **CSTR:** 32038.14.CPB.ae2ebe

1. Introduction

Spin-transfer torque magnetoresistive random access memory (STT-MRAM) is emerging as a promising non-volatile memory technology characterized by low power consumption and high performance. The core structure of STT-MRAM consists of magnetic tunnel junctions (MTJs), typically composed of two ferromagnetic (FM) layers separated by a thin insulating barrier, as illustrated in Fig. 1(a). The fundamental operating principle of STT-MRAM relies on spin-transfer torque (STT), which induces magnetization switching in nanostructured magnetic materials through spin-polarized currents.[1,2] However, the practical performance of spintronic devices, including MTJs, is significantly influenced by magnetization noise.[3–6] Particularly, under thermally activated switching conditions, thermal noise becomes the dominant factor due to its pronounced effect on modifying the effective temperature and lowering the energy barrier for magnetization reversal.[7] The crucial consequence of thermal noise is the reduction of the energy barrier required for magnetization switching. When the applied current pulse approaches the critical switching current of the MTJ, thermal noise enables probabilistic magnetization switching. Such probabilistic behavior of MTJs facilitates their application in probabilistic computing.

Thermal noise is thus not merely a disturbance but an intrinsic physical mechanism that fundamentally governs the stochastic behavior of nanoscale magnetic systems. In contrast to other extrinsic sources of randomness, such as structural imperfections or current fluctuations, thermal noise arises naturally from temperature-dependent spin fluctuations and can be accurately described within the stochastic Landau–Lifshitz–Gilbert framework. This intrinsic origin makes thermal noise both unavoidable and exploitable — it not only limits the deterministic reliability of magnetic switching but also provides a controllable route to realize probabilistic switching near the critical current threshold. Therefore, understanding the quantitative influence of thermal noise on the switching probability is essential for both improving the stability of spintronic memory devices and harnessing stochasticity for probabilistic and neuromorphic computing. In this work, we systematically investigate thermal-noise-induced probabilistic switching in spin-transfer torque magnetic tunnel junctions (STT-MTJs) using a physics-based spin-circuit simulation framework. The results reveal clear transitions between deterministic, mixed, and thermal-noise-dominated regimes, offering new insights into how intrinsic thermal fluctuations shape magnetization dynamics and device functionality.

2. Method

This work utilizes a physics-based simulation framework implemented entirely in SPICE for hybrid spintronic and conventional electronic circuits.[8] To investigate proba-

[†]Corresponding author. E-mail: hushaojie@sztu.edu.cn

© 2026 Chinese Physical Society and IOP Publishing Ltd. All rights, including for text and data mining, AI training, and similar technologies, are reserved.

bilistic switching in MTJs induced by thermal noise, we developed a spin circuit comprising an MTJ module, two non-ferromagnetic (NM) modules, and a Landau–Lifshitz–Gilbert (LLG) module, as shown in Fig. 1(b). The MTJ block, structured as a nanopillar, is positioned between two NM modules, each with a radius of 75 nm. The magnetic free layer within the MTJ has a thickness of 1.6 nm. All simulations including thermal noise were performed at room temperature (300 K). Additional room temperature parameters are listed in Table 1. In this study, the magnetic free layer is modeled as a single-layer ferromagnetic film with perpendicular magnetic anisotropy (PMA), which is a standard and well-characterized configuration in STT-MRAM devices. The present work focuses on the intrinsic effect of thermal noise on probabilistic switching, and thus interfacial coupling effects are not included in this simulation. The magnetization orientation of the free layer is denoted by θ, representing the angle between the $+\hat{z}$ axis and the instantaneous magnetization direction $\hat{m}$. Figure 1(b) also illustrates a schematic diagram of the spin circuit used to simulate spin current transport within the device. The employed LLG equation can be expressed as follows:

$$\left(\frac{1+\alpha^2}{\gamma H_{\rm K}}\right)\frac{{\rm d}\hat{m}}{{\rm d}t} = -\hat{m}\times h_{\rm eff} - \alpha\times\hat{m}\times(\hat{m}\times h_{\rm eff}) - \alpha\times\hat{m}\times(\hat{m}\times\hat{i}_{\rm s}) + \alpha\hat{m}\times\hat{i}_{\rm s}, \quad (1)$$

where α is the damping coefficient, γ is the gyromagnetic ratio, $\hat{m}$ is the time-dependent magnetization (unitless), $h_{\rm eff}$ is the normalized effective field $\hat{H}_{\rm eff}/H_{\rm K}$, $\hat{H}_{\rm eff} = \hat{H}_{\rm K} + \hat{H}_{\rm p} + \hat{H}_{\rm ext}$, including uniaxial and shape anisotropy as well as the external magnetic field, and $i_{\rm s}$ is the normalized spin current $\hat{I}_{\rm s}/H_{\rm K}$. $\hat{I}_{\rm s} = \frac{\hbar I}{2qM_{\rm s}V}$, and I is the spin-polarized charge current flowing to the magnetic free layer. q is the value of the electron charge, and V is the volume of the magnetic free layer.

Table 1. Parameters for the simulation.

Description	Parameter	Value
Saturation magnetization	$M_{\rm s}$	9×10^5 A/m[9]
Uniaxial anisotropy constant	$H_{\rm K}$	8×10^4 A/m[9]
Damping coefficient	α	0.03[9]
Gyromagnetic ratio	γ	1.76×10^{11} rad(s·T)$^{-1}$
Radius of pillar	r	75×10^{-9} m[10]
Resistivity of NM	$\rho_{\rm NM}$	2.89×10^{-8} Ω·m
Conductance of junction	G_0	3.77×10^{-3} Ω^{-1}
Free layer spin polarization	P_1	0.46
fixed layer pin polarization	P_2	0.46
Spin diffusion length of NM	$\lambda_{\rm NM}$	450×10^{-9} m[11]
Spin diffusion length of FM	$\lambda_{\rm FM}$	2×10^{-9} m[12]
Thickness of fixed layer	$t_{\rm FM}$	1.6×10^{-9} m
Thickness of NM	$t_{\rm NM}$	200×10^{-9} m

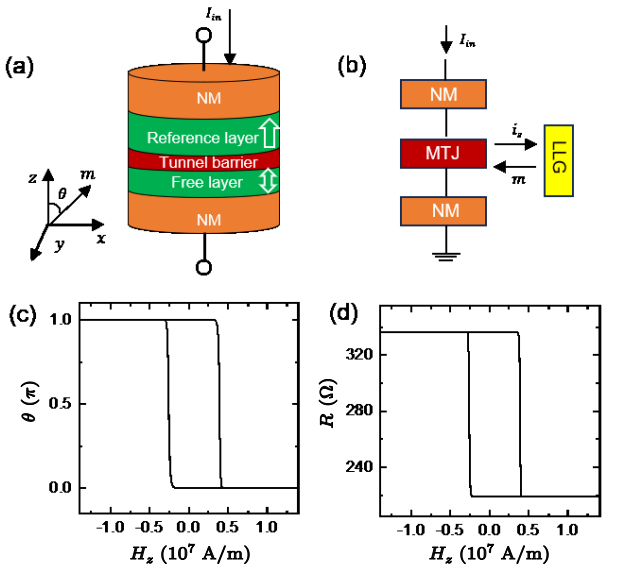


Fig. 1. (a) The schematic structure of the STT-MTJ consists of an MTJ sandwiched between two non-ferromagnetic layers, and the θ angle is defined as the angle between the magnetization directions of the free and fixed layers. (b) Spin-circuit model of the STT-MTJ. (c) The variation of the θ angle with the applied magnetic field. (d) The variation of the MTJ resistance with the applied magnetic field.

3. Result and discussion

To validate the fundamental operation of the MTJ, simulations were conducted on the magnetization switching of the free layer by sweeping an external magnetic field along the z-direction. Figures 1(c) and 1(d) plot the magnetization angle θ of the free layer and the MTJ resistance, respectively, as functions of the external magnetic field. As the external magnetic field magnitude decreases from positive values, the magnetization of the free layer switches from the $+z$ to the $-z$ direction, transitioning the MTJ from a parallel (P) to an antiparallel (AP) state. Correspondingly, the MTJ resistance increases from its initial value of approximately 220 Ω to 340 Ω, as illustrated in Fig. 1(d). When sweeping the magnetic field back from negative maximum values toward positive values, the magnetization of the free layer returns to the $+z$ direction at a specific positive magnetic field, and the MTJ resistance reverts to its initial lower value. The tunneling magnetoresistance (TMR) ratio calculated from these simulations is approximately 54.5%, given by TMR $= (R_{\rm AP} - R_{\rm P})/R_{\rm P}$. The MTJ conductance can be theoretically described by

$$G = G_0[1 + P_1P_2\cos(\theta)], \quad (2)$$

where G_0 is the baseline conductance of the junction, and P_1 and P_2 represent the spin polarizations of the free and fixed layers, respectively. It should be emphasized that a higher spin polarization leads to an increased TMR ratio and a modest reduction in the critical switching current density, but the overall thermally induced probabilistic switching characteristics remain unchanged.

The STT-induced switching behavior was investigated under varying pulse current densities without thermal noise. The applied current pulses had a duration of 20 ns, with the total simulation duration set to 100 ns. To better illustrate the switching dynamics, Fig. 2(a) presents a color map of the magnetization angle θ versus current density and time. At low current densities, such as 3.42×10^{11} A/m^2, the magnetization fails to switch, as shown in Fig. 2(b). Prior to full magnetization reversal, a narrow region with rapid precessional dynamics appears. With increasing current density, the reversal time markedly decreases, reaching a minimum reversal time of about 5 ns. These simulation results closely align with the dynamic characteristics observed experimentally in STT-MRAM devices.

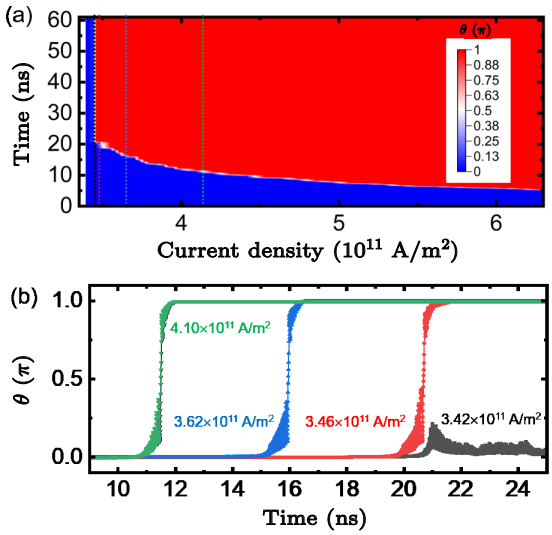


Fig. 2. (a) The color map of θ as a function of time and current density. (b) The time dependence of θ for the MTJ free layer at various current densities.

The influence of thermal noise on magnetization switching in MTJs was investigated by introducing thermal fluctuations modeled as a white-noise effective magnetic field into the LLG equation. The effective thermal noise field can be expressed as follows:[4]

$$H = \sqrt{\frac{4K_{\mathrm{B}}T\alpha f}{\gamma M_{\mathrm{s}} H_{\mathrm{K}}}}, \tag{3}$$

where K_{B} is the Boltzmann constant, T is the absolute temperature, and f is the attempt frequency. It should be noted that the resistive (current-induced) thermal noise was not treated as an independent contribution, as its impact on the switching statistics is minimal under our simulation conditions.

To assess the impact of thermal fluctuations, the temporal evolution of the magnetization angle under various current densities at a pulse duration of 20 ns is presented in Fig. 3(a). Notably, the applied current densities are significantly below the deterministic switching current density of 3.46×10^{11} A/m^2. However, probabilistic switching begins to occur at a current density of 2.33×10^{11} A/m^2, with a 1% switching probability, and achieves a 100% switching probability at a current density of 2.68×10^{11} A/m^2. Conversely, when the pulse duration is shortened to 0.2 ns, probabilistic switching behavior is no longer observed, regardless of the increased current density, as demonstrated in Fig. 3(b). This outcome highlights that current density primarily governs magnetization reversal under short pulse durations, with thermal noise exerting negligible influence.

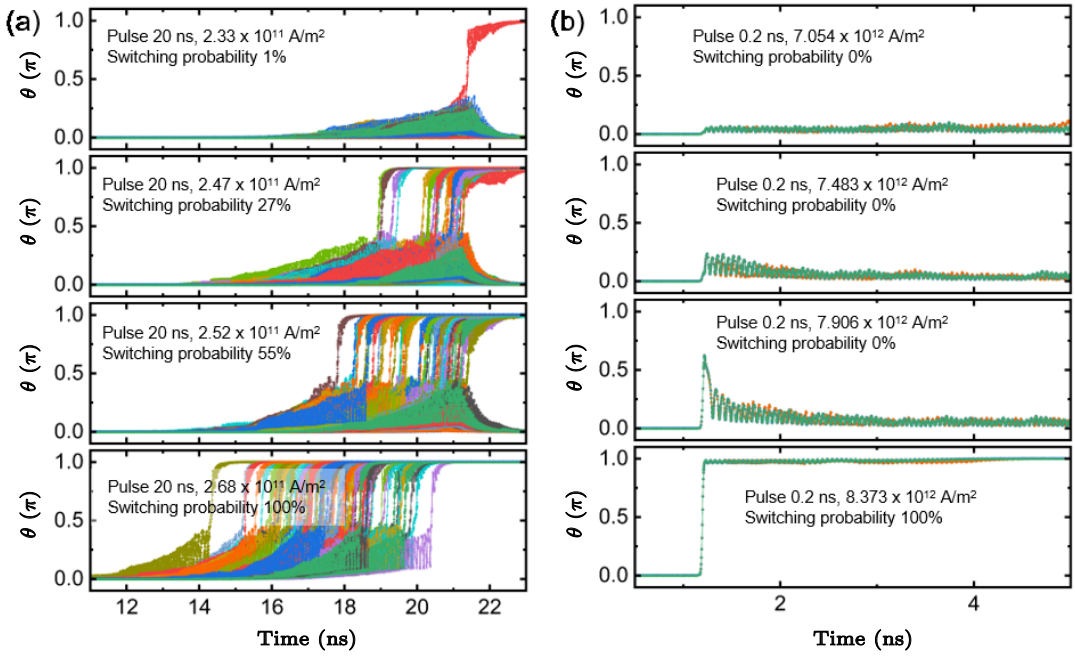


Fig. 3. (a) The time dependence of the magnetization angle under various current densities with a pulse duration of 20 ns, considering thermal noise over 100 simulation runs. (b) The time dependence of the magnetization angle under various current densities with a pulse duration of 0.2 ns, considering thermal noise over 100 simulation runs.

To elucidate the distinct mechanisms involved, Fig. 4(a) provides a contour plot illustrating the switching probability as a function of current density and pulse duration. For pulse durations exceeding approximately 10 ns, a pronounced transitional region (white region) emerges between 0% and 100% switching probabilities, clearly indicating the dominant role of thermal noise in probabilistic magnetization reversal. We have also performed additional simulations varying M_s, H_K, and α. The probabilistic switching window remains qualitatively unchanged, although the threshold current shifts. These results confirm that the observed probabilistic switching is robust against moderate parameter variations. In contrast, at pulse durations shorter than 1 ns, the switching probability exhibits an abrupt transition directly from 0% to 100% with increasing current density. This switching behavior aligns well with theoretical predictions of deterministic magnetization switching processes in MTJs. Additionally, within intermediate pulse durations (approximately 1–10 ns), the probability transition from 0% to 100% is abrupt yet influenced by thermal fluctuations, reflecting a combined effect of current density and thermal noise. This also indicates that the mixed regime (1–10 ns) can be interpreted as a partially thermally activated process. Magnetization precession reduces the effective energy barrier, allowing thermal fluctuations to assist switching with a finite probability. This explanation aligns with Fokker–Planck analyses.[6,13]

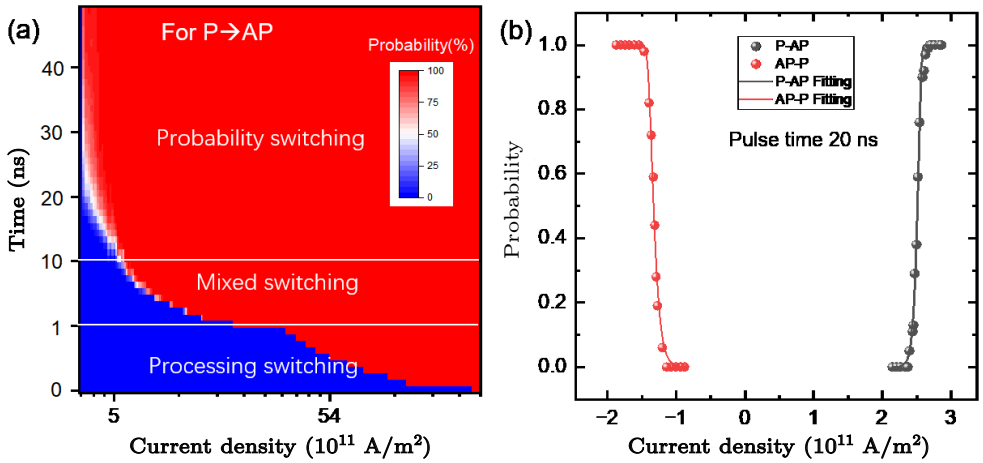


Fig. 4. (a) The relationship between the switching probability of the magnetic moment in the MTJ free layer and the current density and pulse duration under thermal noise. (b) The switching probability of the MTJ free layer under different current densities with a pulse duration of 20 ns. The red curve indicates that the initial state of the MTJ is an antiparallel state (AP), while the black curve indicates that the initial state of the MTJ is a parallel state (P). The solid dots represent the simulation results. The solid lines represent the fitting results obtained using a heuristic equation.

The switching probabilities at varying current densities for different initial magnetization states are depicted in Fig. 4(b). When the MTJ is initially in a parallel state, the switching probability begins to rise at a positive current density of 2.37×10^{11} A/m^2, reaching 100% at approximately 2.44×10^{11} A/m^2. Conversely, when the initial state is antiparallel, magnetization switching initiated by a negative current starts at a lower current density of 1.07×10^{11} A/m^2, achieving a 100% probability near 1.45×10^{11} A/m^2. This notable asymmetry in switching currents and transition widths arises primarily from heat generation due to spin-current scattering within the tunneling barrier.[14] The calculated switching probability aligns well with the heuristic model described by the following equation:[13,15]

$$P = 1 - \exp\left\{-\frac{t}{\tau}\exp[-\Delta(1 - I_{sw}/I_C)]\right\}, \tag{4}$$

where t represents the duration of the applied switching current pulse (20 ns in our simulations), Δ denotes the magnetic memory energy barrier, and τ is the inverse of the attempt frequency. The critical switching current I_C corresponds to the minimum current required to switch the MTJ resistance within the specified pulse width t. To examine temperature effects, we performed additional simulations at 250 K and 350 K. As expected, higher temperatures broaden the sigmoidal transition window, while lower temperatures sharpen it. The general trend agrees with thermally activated switching theory.

4. Conclusion

In this study, we analyzed how thermal noise affects probabilistic switching in STT-MTJs using spin-circuit simulations. Thermal noise strongly impacts switching for pulse durations over 10 ns, resulting in probabilistic switching, while pulses under 1 ns show deterministic switching with minimal thermal effects. Pulses between 1–10 ns exhibit mixed behaviors, reflecting partial thermal influence. Our results confirm the reliability of the simulation model and offer a foundation for future MTJ applications, such as true random number generators and neuromorphic computing.

Acknowledgments

Project supported by Shenzhen Science and Technology Program (Grant No. JCYJ20240813113228037), Natural Science Foundation of Top Talent of SZTU (Grant Nos. GDRC202510 and GDRC202323), Key Discipline Construction Project of Guangdong Province (Grant No. 2022ZDJS110), Shenzhen Fundamental Research Fund (Grant No. JCYJ20220818102214030), Key Colleges and Universities Project of Guangdong Province (Grant No. 2023ZDZX1019), and Engineering Research Center of Guangdong for Compound Semiconductor Devices and Chips.

References

[1] Slonczewski J C 1996 *J. Magn. Magn. Mater.* **159** L1
[2] Sun J Z 2000 *Phys. Rev. B* **62** 570
[3] Wang X, Zheng Y, Xi H and Dimitrov D 2008 *J. Appl. Phys.* **103** 034507
[4] Brown W F 1963 *Phys. Rev.* **130** 1677
[5] Urazhdin S, Birge N O, Pratt W P and Bass J 2003 *Phys. Rev. Lett.* **91** 146803
[6] Bedau D, Liu H, Sun J Z, Katine J A, Fullerton E E, Mangin S and Kent A D 2010 *Appl. Phys. Lett.* **97** 262502
[7] Wang Y, Zhou Y and Zhang F C 2013 *Appl. Phys. Lett.* **103** 022403
[8] Camsari K Y, Ganguly S and Datta S 2015 *Sci. Rep.* **5** 10571
[9] Wang Z, Zhao W, Deng E, Klein J O and Chappert C 2015 *J. Phys. D: Appl. Phys.* **48** 065001
[10] Wang M, Cai W, Zhu D, Wang Z, Kan J J, Zhao Z, Cao K, Wang Z, Zhang Y, Zhang T, Park C, Wang J, Fert A and Zhao W 2018 *Nat. Electron.* **1** 582
[11] Hu S, Itoh H and Kimura T 2014 *NPG Asia Mater.* **6** e127
[12] Cui X, Hu S and Kimura T 2022 *J. Phys. D: Appl. Phys.* **55** 165004
[13] Koch R H, Katine J A and Sun J Z 2004 *Phys. Rev. Lett.* **92** 088302
[14] Liu S and Hu S 2021 *IEEE Trans. Magn.* **58** 1
[15] Wang P, Zhang W, Joshi R, Kanj R and Chen Y 2012 *Proc. Int. Conf. Comput.-Aided Des. (ICCAD)* pp. 720